21, rue d'Artois, F-75008 PARIS
http : //www.cigre.org

CIGRE US National Committee
2014 Grid of the Future Symposium

# Evaluation of Meshed Distribution Systems for Increased Penetration of Distributed Generation

**M. DAVOUDI[1], V. CECCHI[1], J.R. AGUERO[2]**
**[1] University of North Carolina at Charlotte, [2] Quanta Technology**

## SUMMARY

Utility distribution grids in the US are experiencing proliferation of Distributed Generation (DG) largely due to the need to comply with goals set by Renewable Portfolio Standards (RPS), the availability of economic incentives, and technology cost reductions. Interconnecting properly-sized DG units at strategic locations in the distribution grid may lead to important benefits and improve power delivery efficiency (e.g., reduce technical losses, shave peaks, etc). However, very high penetration levels of DG may cause significant impacts on the distribution system (voltage increase, reverse power flows, etc).

The large majority of US distribution grids have been traditionally operated in a radial manner. Radial operation requires simpler planning and engineering approaches and less expensive equipment. However, it is less efficient from a reliability and power quality standpoint and leads to greater voltage drops and power losses on distribution lines. Furthermore, radial operation may also limit the ability of distribution grids to host higher penetration levels of DG. As distribution grids evolve into highly dynamic active systems it is necessary to explore alternative operation approaches that facilitate adoption and higher penetration levels of DG. In this regard, and using the transmission and sub-transmission grids as inspiration, meshed operation of distribution grids has enough merits to be considered as a potential solution for integrating growing amounts of renewable generation. The advent of smart grid technologies, advances in protection systems and distribution automation, and increased interest in interconnection of DG have paved the way to look at this operation approach.

In this paper, first, the maximum allowable DG generation in the distribution grid is estimated based on allowable steady-state voltage and current limits, i.e. the DG penetration at a specific bus should not cause the bus voltages or the line currents in the system to violate their acceptable operating or planning limits. This maximum value is then compared for radial and meshed operation of a 69 bus test system, for different DG operation modes (unity, inductive and capacitive power factors[1]). Cases with multiple DGs installed at different buses in the

---

[1] The literature usually refers to DG power factors as unity, leading and lagging. Since the convention for *generation* power factor is the opposite of that of loads, these terms sometimes cause confusion among readers (i.e., a generator operating under leading power factor absorbs VARs from the grid while a load with leading power factor injects VARs to the grid). For this reason in this paper the terms

mghiafeh@uncc.edu

distribution system are also studied in this paper. Results of the analyses show that, based on metrics of steady-state bus voltage and line current limits, a properly-chosen distribution system meshed configuration may increase the allowable maximum penetration of DG. Moreover, an inductive power factor operation mode is shown to allow higher penetration levels of DG, since the absorbed reactive power decreases bus voltages.

The paper is organized as follows: Section 1 introduces the subject in more detail, Section 2 presents the method used for determining the maximum allowable generation in a given grid configuration, Section 3 presents the test case and results, and Section 4 discusses the conclusions of the study and outlines potential future work.

## KEYWORDS

Distributed Generation- Meshed Operation- Proliferation- Penetration Level- Radial Feeder

## 1. Introduction and Background

Integrating DGs in the network, if properly sized and located, can have advantages for the system. Voltage profiles can be improved [1], overall system losses can be reduced [2] [3], deferment of investment in the system can be achieved [4], etc. However, DGs can also have negative impacts on the network. For example, increasing the penetration level above a certain limit might cause overvoltages [2], increase in system losses [3], reverse power flow and its effect on voltage regulators and so on. Environmental and societal concerns are leading toward higher penetration levels of DGs in the distribution networks. However, in high penetration levels of DGs, the network might need reinforcements to withstand these amounts of generation. Meshed network configuration might be a solution for maximizing grid's ability to integrate large amounts of renewable and distributed generation. Although this configuration requires more complex planning and operation and updates to the protection system, it also has several advantages, such as increase in reliability, decrease in system losses and improvement in voltage profile and preventing the overloading of transformers and lines [2]-[6]. Meshed configuration of the network could be chosen such that the negative impacts of meshed operation are omitted or decreased, and the positive effects could be exploited.

Limiting factors to the increased penetration levels of DGs include violations of bus voltage and line current limits, interaction with voltage regulators and control schemes, and effects on the correct operation of protection systems. Increasing the DG penetration level generally improves the voltages in the system which may be desirable at end-of-the-feeder buses; however, the amount of voltage increase should not exceed the steady state limitations on the buses. In some cases, like inductive mode of operating the DG, the voltage might be decreased as a result of reactive power absorption. Therefore, the minimum steady state voltage limit should also be considered. Moreover, as a result of power injection, currents in the lines will also change and may exceed their loadability limit. Different methods to determine maximum allowable DG penetration level have been proposed. For example, in [7] and [8], the maximum allowable DG injection is determined based on steady state voltage limits. In [9], harmonic distortion levels are used to determine the maximum allowable DG output in the system. In this paper, the maximum allowable DG injection is determined based on the metrics of steady-state voltage and current limits.

---

inductive and capacitive have been chosen to replace leading and lagging *generation* power factors. Here, inductive and capacitive power factors mean absorbing and injecting VARs, respectively.

## 2. Estimation of Maximum Allowable DG Penetration: Steady-State Voltage and Current Limits

In this paper, bus voltages and line currents limits are considered for determining the maximum allowable penetration of DGs in the network. Bus voltage magnitudes should typically be between 0.95 and 1.05 per unit, and line current limits depend on the specifications of conductors used in the system.

Successive power flow methods can be used to determine this maximum allowable injection. In details, in a given system structure, a DG with a minimum possible active power injection is installed at the desired bus where its maximum allowable output is to be calculated. Then, a power flow method is used to calculate bus voltages and hence line currents in the system. If the voltage and current limits are not violated, the DG output at the desired bus can be increased. In each step, all the voltage and current limits are checked so that no violation is occurred, until the DG output reaches its maximum allowable value where if it is increased a single step, at least one violation is seen in either bus voltages or line currents. The successive power flow method is time consuming and has a huge computational burden, since a complete load flow is required for each iteration. This becomes an important issue specifically in distribution networks where the system dimension is larger.

Another method of calculating the maximum allowable DG penetration in a system is sensitivity analysis approach [7], [8], [10]. Consider that the DG is going to be installed at bus *j* of the system, which might already have other DGs connected to it, or might have the substation as its only source. Moreover, during this sensitivity analysis, the structure of the network, either radial or meshed, is fixed.

Running the power flow before connecting the DG at bus *j*, which will be denoted as base case condition, yields to the bus voltage magnitudes and angles in the system. Consider the Jacobian matrix, the changes in active and reactive powers of the buses, and resulting changes in the voltage magnitudes and angles in the following equation:

$$\begin{bmatrix} \Delta P \\ \Delta Q \end{bmatrix} = \begin{bmatrix} J_1 & J_2 \\ J_3 & J_4 \end{bmatrix} \begin{bmatrix} \Delta \delta \\ \Delta V \end{bmatrix} \tag{1}$$

Therefore, one can write the equation between changes in voltage magnitudes due to active power changes in the system when $\Delta Q$ is zero, and also due to reactive power changes in the system when $\Delta P$ is zero, as follows:

$$\Delta P = \left(J_2 - J_1 J_3^{-1} J_4\right) \Delta V = J_{RPV} \Delta V \tag{2}$$

$$\Delta Q = \left(J_4 - J_3 J_1^{-1} J_2\right) \Delta V = J_{RQV} \Delta V \tag{3}$$

Knowing the $\Delta P$ and $\Delta Q$ values, and noticing that based on the power factor of the desired DG at bus *j*, $\Delta Q$ could be expressed in terms of $\Delta P$, the changes in voltage at bus *i* due to power injection at bus *j* can be calculated:

$$\Delta V_i = V_i - V_i^0 = J_{VPQ_{ij}} P_j = P_j \left[ \left(J_2 - J_1 J_3^{-1} J_4\right)^{-1} + \left(J_4 - J_3 J_1^{-1} J_2\right)^{-1} \tan(\cos^{-1}(pf_j)) \right] \tag{4}$$

The base case results will be denoted by a zero superscript, like $V^0$. Note that the voltage change for each bus can be negative or positive based on the values of Jacobian matrix. As mentioned earlier, power flow is required to be performed only once in this method. The values of changes mentioned in above equations are actually the changes from the base case results and are easily calculated knowing the power flow results. Hence, for all system buses, the maximum allowable value of $\Delta V_i$ is determined. Using (4), one can calculate the maximum value of $P_j$ allowed before a violation in voltage at each bus in the system occurs. This will yield to *n-1* values of $P_j$, where *n* is the size of the system. Then, the minimum value of $P_j$ is selected since no violations are allowed in system voltages. Unlike the repetitive power flow method, this approach uses closed form equations and does not require repetition. Since DG capacities are limited, the calculated value for allowable power injection should also consider this limit. Moreover, in this paper, the total amount of DG power injection was also limited to not exceed the total load of the system. Therefore, the maximum allowable DG injection at bus *j* which satisfies voltage limits and also these two latter limitations is denoted by $P_j^{Max,V,DG}$.

The next step consists of setting the DG output power at bus *j* to $P_j^{Max,V,DG}$ and determining bus voltage magnitudes and angles. Instead of running power flow to determine the updated voltages, a different approach is used here to reduce computational burden. The changes in the voltage magnitudes due to $P_j^{Max,V,DG}$ output from the DG are calculated using (4) and the voltage magnitudes are updated. A similar equation to (4) can be obtained for relating changes in voltage angles due to a DG and the DG power injections [10]. Hence, voltage angles can also be updated from the base case results. After updating voltage magnitudes and angles, line currents are calculated to see if they are within the acceptable operating limits. If the values of the line currents are also in the desired limits, the final result for maximum allowable DG penetration is achieved as $P_j^{Max,Total}$. Otherwise, the penetration level is decreased in steps until the currents criteria are also met.

The described procedure can be used to find the maximum allowable penetration of a DG which is going to be added to a certain bus regardless of the configuration of the network. In the next section, different scenarios will be studied for a specified test system. Results for radial and meshed configurations for different DG power factors and for cases with multiple DGs will be presented.

## 3. Evaluation studies

The test case used in this section is a 69 node 12.66 kV test system, as shown in Fig. 1, with the detailed information as described in [11] and [12]. Total active and reactive power load of this system are 3.802 MW and 2.694 MVar, respectively, and the voltage at the substation is set to 1.04 per unit to maintain all voltages in the desired range of 0.95 pu and 1.05 pu. As shown in Fig. 1, the system has 5 tie lines that could be added to the network to form meshed structures. The meshed structure obtained by closing the tie switch $T_1$ is denoted by meshed case $C_1$ in this paper. Since the total load of the system is 3.802 MW, the DG capacities are indicatively limited to 4 MW.

### *3.1. Effects of different DG power factors and distribution grid configurations*

Consider that no DGs are currently connected to the system, and the maximum allowable DG injection at bus 27 is to be calculated. Using the proposed method as presented in the previous section, the maximum power output of a DG working in unity power factor connected to this bus which does not violate the voltage limits is 0.908 MW. If the repetitive power flow method was used, this value was obtained as 0.958 MW, which shows good accuracy of the proposed method with 5.2% absolute error percentage. All conducted studies have shown that the proposed method is conservative for calculating the maximum allowable penetration value. Fig. 2a shows the voltages of the system in case of having the DG connected to bus 27 for different values of output power with unity power factor when the system is operated radially. As can be seen in this figure, the voltages are gradually increased while the output of this DG is increased, and when the output power reaches the calculated value of $P_{27}^{Max,V,DG}$, voltage limits are violated. This figure also verifies the result obtained by the proposed method for $P_{27}^{Max,V,DG}$. Then, currents in the network are calculated in case of having the DG. Since no violation is occurred, the final value for $P_{27}^{Max,Total}$ is 0.908 MW. Now consider operating the system in the meshed configuration $C_2$ - closing tie switch $T_2$; in this case, the value of $P_{27}^{Max,Total}$ would be 2.304 MW, which shows an increase of 199%. The voltages of the buses for different values of injected power at bus 27 with unity power factor when the system is operated in meshed configuration $C_2$ are shown in Fig. 2b, which verifies the obtained value for the $P_{27}^{Max,Total}$ in this operating scenario.

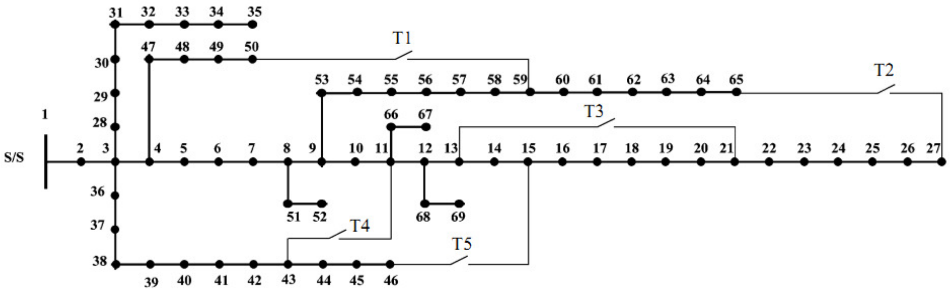

Fig. 1. Test system.

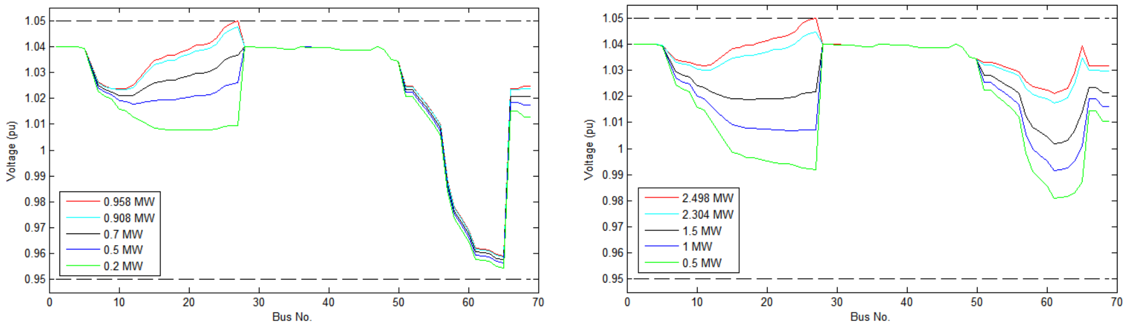

a)

b)

Fig. 2. Bus voltages for different power injections at bus 27 in a) radial case and b) meshed case $C_2$.

The procedure for obtaining the maximum allowable active power injection is the same for different DG power factors. However, since the DG also injects reactive power in capacitive mode of operation, the voltages increase more in comparison to the unity power factor case. Therefore, it is expected that the maximum allowable penetration of a DG in a certain bus, when it is operated in capacitive mode, would be less than the unity power factor. A similar discussion is also valid for the general trend that the inductive mode of DG operation allows more power injection, since the DG absorbs reactive power and this absorption reduces the voltages. However, this might not always be the case, since with increasing the absorbed reactive power, some voltages might violate the lower operating thresholds. Fig. 3

demonstrates the maximum allowable active power injection at all buses of the system in different structures for power factor of DG equal to unity, 0.9 inductive, and 0.9 capacitive. As can be seen, results of the study show that in general, meshed operation scenarios can allow higher penetration levels of DG in the system.

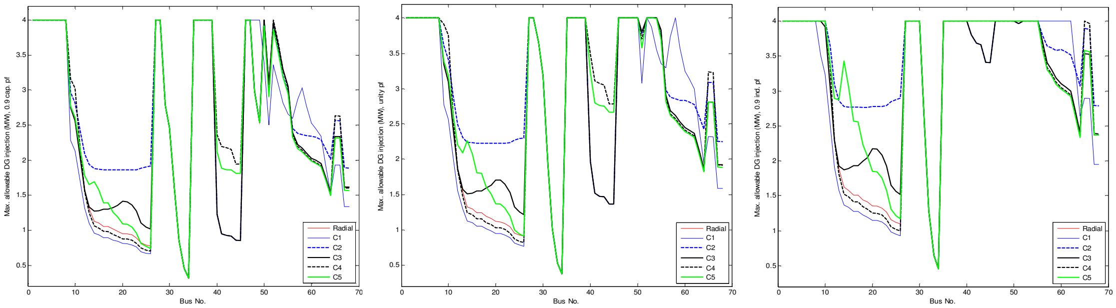

a) 0.9 capacitive b) unity c) 0.9 inductive

Fig. 3. Maximum allowable power injection in all buses of the system in different operating scenarios for different power factors of operating the DG.

Up to now, the effect of adding one DG at the system has been analyzed. To compare different modes of operating the DG and different structures of the system, the maximum allowable DG penetration of all buses of the system, each calculated individually, are averaged to represent as an index for each "system structure- DG power factor" case. The results are provided in Table 1, and show that the average value for $P_j^{Max,Total}$ is increased for meshed structures in most cases. The previous discussion on the effects of DG power factor is also verified in this table. It is to be noted that the results for maximum allowable injection have shown that in the case with 0.8 inductive power factor, the generation at more buses is limited due to the current limits. Therefore, for this case, the results in Table 1 show a lower increase in comparison to the increase seen moving from unity power factor to 0.9 inductive power factor. This is due to the fact that for this inductive power factor, the DG absorbs higher values of inductive power. This, in some cases, increases the current magnitudes in the lines near the bus that has the DG. Therefore, line current limits might be violated in this scenario, which decreases the maximum allowable DG injection in the system.

For example, the value of $P_{52}^{Max,V,DG}$ for the radial structure in case of unity power factor, inductive power factor of 0.9, and inductive power factor of 0.8 is 3.806 MW, 4 MW, and 4 MW, respectively. However, when the DG is generating 4 MW in 0.8 inductive mode, the current limits are violated. The value of $P_{injected}$ is reduced until no violations happen, which is when the DG generates 3.51 MW.

Table 1. Average max. allowable power injection in the system for different operating scenarios and DG power factors

| | Average $P_j^{Max,\ Total}$ (MW) | | | | |
|---|---|---|---|---|---|
| | Capacitive | | Unity | Inductive | |
| | pf=0.8 | pf=0.9 | | pf=0.9 | pf=0.8 |
| Radial | 2.152 | 2.315 | 2.616 | 3.050 | 3.124 |
| $C_1$ | 2.102 | 2.281 | 2.597 | 3.036 | 3.086 |
| $C_2$ | 2.380 | 2.566 | 2.926 | 3.439 | 3.550 |
| $C_3$ | 2.205 | 2.374 | 2.962 | 3.154 | 3.252 |
| $C_4$ | 2.264 | 2.422 | 2.759 | 3.073 | 3.135 |
| $C_5$ | 2.258 | 2.428 | 2.799 | 3.231 | 3.392 |

Maximum allowable power injection in unity power factor of DG for the buses located at the end of laterals are calculated for different modes of operating the network, as shown in Fig. 4. The following observations can be made:

- Each meshed configuration might have different impact on maximum allowable generation at different buses. For example, while meshed configuration $C_4$ allows the highest amount of $P_{67}^{Max,Total}$, it even decreases the amount of $P_{27}^{Max,Total}$ in comparison to the radial case.
- The meshed configuration that allows the most amount of power generation is not the same for all buses. For example, the optimum configuration for bus 46 is $C_5$, while it is $C_2$ for bus 65.
- Therefore, the best meshed configuration of the network should be selected to have the maximum allowable power injection at the desired bus.

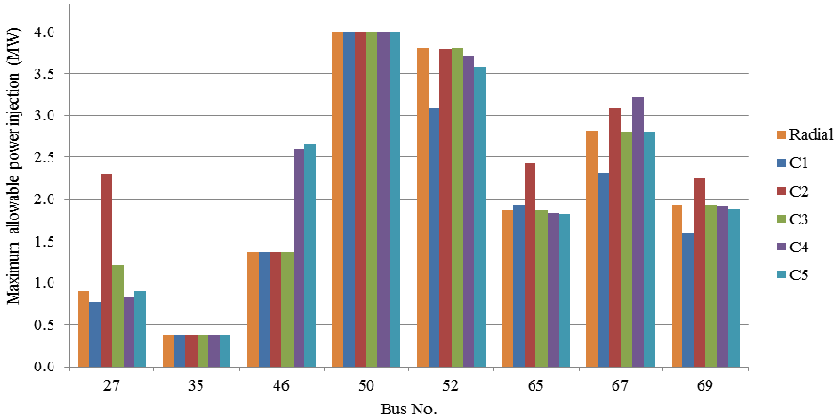

Fig 4. Max. allowable power injection in unity power factor of the DG for end-lateral buses.

### *3.2. Cases with Multiple DGs*

The superior behavior of meshed operation will also be verified in multi-DG scenarios. In these scenarios, the system already has a DG connected to one bus or more, and the maximum allowable power injection at another bus is calculated. For simplicity, the unity power factor is considered for the DGs that are being studied in this section. The results for values of $P_j^{Max,Total}$ for end-lateral buses when the system already has a power injection of 1 MW at bus 65 are shown in Table 2. The results for radial operation mode are shown in MW, where the results for meshed cases are also normalized based on these values and shown in percentage. As can be seen in this table, some conditions allow significant increase of injected power in the network.

This significant feature is also seen when the DG at bus 65 is generating its maximum allowable power in the radial case, which is 1.871 MW. It is to be noted that since the effect of changing the network structure is to be studied here, the amount of power injection at bus 65 is kept constant although the maximum allowable injection at this bus is different for each network structure. The results of $P_j^{Max,Total}$ for end-lateral nodes when the DG at bus 65 is operating at 1.871 MW are presented in Table 3, which also verifies the advantage of the meshed structure in this respect.

As another multi-DG scenario, consider the system with DG at bus 65 generating 1.871 MW in unity power factor, and at bus 27 with 0.69 MW (this is the minimum value in Table 3 for all radial and meshed structures when DG at bus 65 is generating 1.871 MW, and has been selected to make the comparison feasible). Table 4 shows the results of maximum allowable active power generation in other end-lateral buses in unity power factor in this condition, for different network structures. As can be seen from Tables 3 and 4, the operator can choose the meshed scenarios where the allowable generation limit in the specifically desired end-lateral bus is more than other cases. From another perspective, if the structure is determined, the best bus to have the third DG can be chosen. In any case, results shows that if the meshed structure is chosen properly, it generally allows higher penetration levels of DGs in the network.

Table 2. Max. allowable power injection in end-lateral buses in case of having a DG located at bus 65 generating 1 MW

| | $P_j^{Max,Total}$ (MW) | | | | | | Inc % in $P_j^{Max,Total}$ with respect to Radial case | | | | |
|---|---|---|---|---|---|---|---|---|---|---|---|
| Bus No. | Radial | $C_1$ | $C_2$ | $C_3$ | $C_4$ | $C_5$ | $C_1$ | $C_2$ | $C_3$ | $C_4$ | $C_5$ |
| 27 | 0.804 | 0.734 | 1.521 | 1.057 | 0.749 | 0.849 | -8.65 | 89.18 | 31.49 | -6.80 | 5.56 |
| 35 | 0.373 | 0.373 | 0.373 | 0.373 | 0.373 | 0.373 | 0.00 | 0.00 | 0.00 | 0.00 | 0.00 |
| 46 | 1.363 | 1.363 | 1.363 | 1.363 | 2.576 | 2.524 | 0.00 | 0.00 | 0.00 | 89.04 | 85.21 |
| 52 | 3.117 | 2.817 | 3.111 | 3.115 | 3.060 | 2.918 | -9.63 | -0.17 | -0.06 | -1.81 | -6.39 |
| 67 | 2.369 | 2.151 | 2.448 | 2.366 | 2.806 | 2.372 | -9.17 | 3.37 | -0.09 | 18.45 | 0.14 |
| 69 | 1.644 | 1.483 | 1.749 | 1.642 | 1.689 | 1.628 | -9.77 | 6.38 | -0.11 | 2.75 | -0.96 |

Table 3. Max. allowable power injection in end-lateral buses with a DG located at bus 65 generating 1.871 MW ( $P_{65}^{Max,Total}$ )

| | $P_j^{Max,Total}$ (MW) | | | | | | Inc % in $P_j^{Max,Total}$ with respect to Radial case | | | | |
|---|---|---|---|---|---|---|---|---|---|---|---|
| Bus No. | Radial | $C_1$ | $C_2$ | $C_3$ | $C_4$ | $C_5$ | $C_1$ | $C_2$ | $C_3$ | $C_4$ | $C_5$ |
| 27 | 0.721 | 0.705 | 0.801 | 0.930 | 0.692 | 0.803 | -2.32 | 11.00 | 28.88 | -4.06 | 11.37 |
| 35 | 0.373 | 0.373 | 0.373 | 0.373 | 0.373 | 0.373 | 0.00 | 0.00 | 0.00 | 0.00 | 0.00 |
| 46 | 1.362 | 1.362 | 1.362 | 1.362 | 2.415 | 2.419 | 0.00 | 0.00 | 0.00 | 77.32 | 77.54 |
| 52 | 1.760 | 2.601 | 2.546 | 1.757 | 1.546 | 1.357 | 47.84 | 44.70 | -0.16 | -12.12 | -22.90 |
| 67 | 1.646 | 2.019 | 1.912 | 1.644 | 1.891 | 1.481 | 22.62 | 16.13 | -0.16 | 14.88 | -10.06 |
| 69 | 1.423 | 1.402 | 1.325 | 1.421 | 1.511 | 1.426 | -1.47 | -6.87 | -0.13 | 6.19 | 0.22 |

Table 4. Max. allowable power injection in end-lateral buses in case of having a DG located at bus 65 and 27, each generating 1.87 MW and 0.69 MW, respectively

| | $P_j^{Max,Total}$ (MW) | | | | | | Inc % in $P_j^{Max,Total}$ with respect to Radial case | | | | |
|---|---|---|---|---|---|---|---|---|---|---|---|
| Bus No. | Radial | $C_1$ | $C_2$ | $C_3$ | $C_4$ | $C_5$ | $C_1$ | $C_2$ | $C_3$ | $C_4$ | $C_5$ |
| 35 | 0.373 | 0.373 | 0.373 | 0.373 | 0.373 | 0.373 | 0.00 | 0.00 | 0.00 | 0.00 | 0.00 |
| 46 | 1.362 | 1.362 | 1.362 | 1.362 | 0.448 | 0.609 | 0.00 | 0.00 | 0.00 | -67.08 | -55.31 |
| 52 | 0.629 | 0.501 | 0.694 | 1.039 | 0.416 | 1.118 | -20.24 | 10.41 | 65.23 | -33.83 | 77.80 |
| 67 | 0.284 | 0.210 | 0.429 | 0.812 | 0.187 | 1.119 | -26.05 | 51.41 | 186.39 | -34.22 | 294.56 |
| 69 | 0.207 | 0.151 | 0.345 | 0.593 | 0.118 | 0.811 | -27.35 | 66.72 | 186.39 | -43.02 | 291.53 |

## 4. Conclusion

In this paper, the effect of meshing the system on its capability to withhold higher penetration levels of DGs had been analyzed. The simulation results verify that if the meshed structure is chosen properly, the DG output level at a specific desired bus can be improved in comparison to other structures. The presented method can also be used to determine the best bus to connect the DG if the network structure is given. The superior behavior of meshed structure is also seen for multi-DG scenarios, where different buses in the system have DGs. This trend is also seen in different power factor values in inductive and capacitive mode, which is verifying the behavior of meshed structure in allowing higher DG penetration to the network. Future studies will include optimizing the problem as a network reconfiguration approach to choose the best meshed structure possible.

## BIBLIOGRAPHY

[1] C. J. Mozina, “Impact of Green Power Distributed Generation,” IEEE Industry Applications Magazine, pp. 55-62, July- Aug. 2010.

[2] J. R. Aguero, “Improving the Efficiency of Power Distribution Systems through Technical and Non-Technical Losses Reduction,” Transmission and Distribution Conference and Exposition (T&D), Orlando, FL, May 2012.

[3] G. Celli, F. Pilo, G. Pisano, V. Allegranza, R. Cicoria, and A. Iaria, “Meshed vs. Radial MV Distribution Network in Presence of Large Amount of DG,” IEEE Power Systems Conference and Exposition, pp. 709- 714, vol. 2, New York, USA, 2004.

[4] M. E. Baran, H. Hooshyar, Z. Shen, J. Gajda, and K. M. M. Huq, “Impact of High Penetration Residential PV Systems on Distribution Systems,” Power and Energy Society General Meeting, San Diego, CA, July 2011.

[5] V. Cecchi, S. Kamalasadan, J. Enslin, M. Miller, “Grid impacts and mitigation measures for increased PV penetration levels using advanced PV inverter regulation”, Proceedings of the IEEE 2013 Energy Conversion Congress and Exposition (ECCE), Denver, CO, 15-19 Sept. 2013.

[6] T. Chen, W. Huang, J. Gu, G. Pu, Y. Hsu, and T. Guo, “Feasibility study of upgrading primary feeders from radial and open-loop to normally closed-loop arrangement”, IEEE Trans. on Power Sys., vol. 19, no. 3, pp 1308-1316, Aug. 2004.

[7] H. M. Ayres, W. Freitas, M. C. De Almeida, and L. C. P. da Silva, “Method for determining the maximum allowable penetration level of distributed generation without steady-state voltage violations,” IET Generation, Transmission & Distribution, vol. 4, no. 4, pp. 495-508, Apr. 2010.

[8] M. Davoudi, V. Cecchi, J. R. Agüero, “Investigating the ability of meshed distribution systems to increase penetration levels of distributed generation,” Southeastcon, 2014 Proceedings of IEEE , March 2014.

[9] A. Bhowmik, A. Maitra,S. M. Halpin, and J. E. Schatz, “Determination of allowable penetration levels of distributed generation resources based on harmonic limit considerations,” IEEE Trans. on Power Del., vol.18, no.2, pp.619-624, Apr. 2003.

[10] M. Davoudi, V. Cecchi, J. R. Agüero, “Increasing Penetration of Distributed Generation with Meshed Operation of Distribution Systems,” North American Power Symposium (NAPS), 2014, Sept. 2014.

[11] J. S. Savier, and D. Das, “Impact of Network Reconfiguration on Loss Allocation of Radial Distribution Systems,” IEEE Trans. on Power Del., vol. 22, no. 4, pp. 2473-2480, Oct. 2007.

[12] M. E. Baran and F. F. Wu, “Optimal capacitor placement in distribution systems,” IEEE Trans. on Power Del., vol. 4, no. 1, pp. 725–734, Jan. 1989.